http://pubs.acs.org/journal/acsodf
Article

Canny Algorithm Enabling Precise Offline Line Edge Roughness Acquisition in High-Resolution Lithography

Ziyu Hu, Rongbo Zhao, Xiaolin Wang, Peipei Tao, Qianqian Wang, Yimeng Wang, Hong Xu,* and Xiangming He*

Cite This: *ACS Omega* 2023, 8, 3992–3997

Read Online

ACCESS | Metrics & More | Article Recommendations | Supporting Information

ABSTRACT: The line edge roughness (LER) is one of the most critical indicators of photoresist imaging performance, and its measurement using a reliable method is of great significance for lithography. However, most studies only investigate photoresist resolution and sensitivity because LER measurements require an expensive and not widely available critical dimension scanning electron microscopy (SEM) technology; thus, the imaging performance of photoresist has not been adequately evaluated. Here, we report an image processing software developed for offline calculation of LER that can analyze lithographic patterns with resolutions up to ∼15 nm. This software can effectively process all graphic files obtained from commonly used SEM machines by utilizing the adjustable double threshold. To realize the effective detection of high-resolution patterns in advanced lithography, we used SEM images generated from extreme ultraviolet and electron beam lithography to develop and validate the software's graphic recognition algorithm. This image processing software can process typical SEM images and produce reliable LER in an efficient and user-friendly manner, constituting a powerful tool for promoting the development of high-performance photoresist materials.

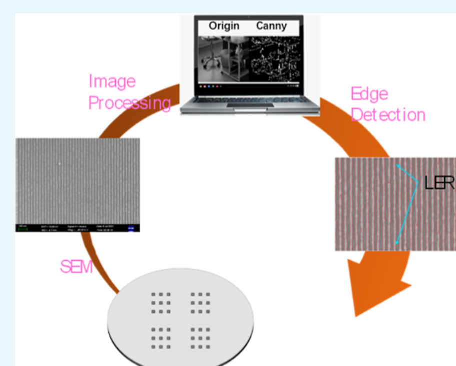

1. INTRODUCTION

Since the world's first integrated circuit was invented in 1958, the number of transistors on a chip has grown from just a few dozen to nearly 100 million transistors/mm^2 in less than 7 decades. Rapid development of chips cannot be achieved without the advancement of photolithography, a process that transfers circuitry from the design layout to the silicon wafer through the principles of optical and chemical reactions. It limits the processing range for other chip processing technologies, so lithography is the key technology driving the development of the chip process. As the core chemical material of the lithography process, the development and research of photoresists are also becoming popular.

In photoresist studies, resolution (R), sensitivity (S), and line edge/width roughness (LER/LWR) are commonly used to characterize the quality of a material. Resolution determines the size of a photolithographic line, and sensitivity determines the necessary exposure dose. The LER/LWR is a parameter that characterizes the extent to which the actual edge deviates from the ideal edge, meaning the degree of defect in the image. The edge roughness is influenced by not only photoresist materials but also the lithography technique. For example, in electron beam lithography (EBL), the scattering of electrons can be far beyond the initial exposure range.[1] Rough edges can significantly affect the quality of the subsequent electronic components, so the LER/LWR is an essential parameter of photoresists.[2,3] These three parameters are often further combined into the Z-factor ($Z = R^3 \times \mathrm{LER}^2 \times S$) for a quick comparison of different photoresists.[4]

The resolution can be obtained by measuring the line width after exposure and development. The exposure dose set during the exposure process yields the sensitivity of the photoresist. However, the measurement of LER requires obtaining the position of several points at the line edge. While the lithographic lines are very narrow, from a few nanometers to tens of nanometers, the location of line edge points is difficult to obtain by general methods. LER/LWR generally requires online measurement using critical dimension scanning electron microscopy (CD-SEM).[5] Unlike the commonly used SEM, CD-SEM is expensive and not widely available; thus, many photoresist studies focus on resolution and sensitivity, with relatively little quantitative analysis of LER/LWR. For example, in Li's study of the effects of particle size and surface groups on nanoparticle photoresists, he evaluated the relationship between the resolution and sensitivity but did not discuss the LER in detail.[6] In a study on the low-voltage three-dimensional EBL process, Xiang mentioned that the process

Received: October 20, 2022
Accepted: December 30, 2022
Published: January 18, 2023

ACS Publications
© 2023 The Authors. Published by American Chemical Society

could obtain a high-precision three-dimensional structure, while this work did not perform quantitative analysis of the LER.[7] However, it can be seen from the equation of the Z-factor that LER is one key parameter in describing the performance of photoresists and its weighting in the Z-factor is even higher than the sensitivity of materials. In addition to lithography, many other nanofabrication techniques face challenges for defect control, especially sub-10 nm fabrications. For example, block copolymer (BCP)-based directed self-assembly (DSA) is considered a promising new semiconductor fabrication technology due to its ability to obtain long-range ordered periodic microstructures.[8] However, defect control and quantitative analysis of defects are critical issues in this field.

Therefore, an efficient and convenient method for measuring LER is highly desired for photoresist development and lithography process research. Offline measurement of LER is a possible solution based on SEM images of lithography patterns.[9] Some commercial software is now able to perform offline LER measurement analysis.[10] Additionally, some scientific institutions have developed software for measuring LER. For example, researchers at the Paul Scherrer Institute have developed a measurement software called SMILE that can calculate LWR.[11] Yazgi et al. developed a calculation software of LER and LWR using the Canny algorithm for edge recognition.[10] However, these methods still present some limitations, such as undisclosed methods, inaccurate edge recognition, and inconsistent calculation results. In this work, we report an offline LER calculation software that employs an image processing algorithm to effectively process all graphic files obtained from commonly used SEM machines. The software implements a double-threshold adjustable Canny edge detection algorithm and can identify edge data with a better match. Additionally, high-resolution patterns obtained from today's advanced lithographic techniques, including electron beam and extreme ultraviolet lithography, are used to develop and validate the software's graphic recognition algorithm.

2. LER/LWR CALCULATION PROCESS

The offline measurement of LER/LWR is mainly divided into two steps: the first step is to use an edge detection algorithm, the Canny algorithm, to extract the edge data of the line patterns from the SEM images. The second step then performs a fractal analysis of the extracted data in terms of amplitude and power spectral density (PSD).

2.1. Canny Algorithm for the Extraction of Edge Data. The calculation of LER or LWR depends on the location of the lithographic line edges in the SEM image. Therefore, it is necessary to identify the edge information in an entire SEM image with interference caused by non-edge points. We use the image edge recognition method to extract the edge position information.

According to the principle of secondary electron imaging, for a smooth specimen surface, the secondary electron yield satisfies eq 1

$$\delta = \frac{I_s}{I_p} \propto \frac{1}{\cos\ \alpha} \tag{1}$$

The secondary electron yield δ, which is the ratio of the intensity of the secondary electron signal I_s to the intensity of the incident electron beam I_p, is inversely proportional to the cosine of the angle α between the surface normal of the sample and the incident electron beam.[12] In Figure 1, we can see that

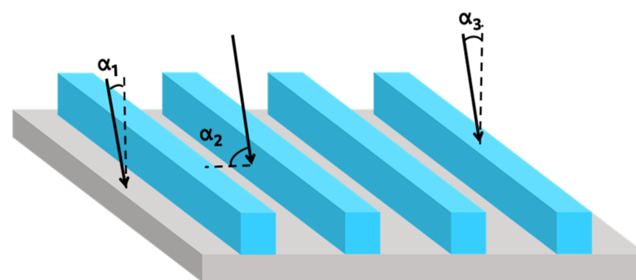

Figure 1. Electron beam incidence in the background, at the edges of the lines, and on the top of the lines.

the angle α at the edge of the line is always larger than the background or the top of the line. Thus, according to eq 1, the brightness of the pixels at the edge is significantly higher than that of the other parts. In image processing, the location of the largest gradient of pixel brightness values in an image is generally recognized as the edge of a pattern. Therefore, the edges of photoresist lines can be screened out by edge detection in theory. In image processing, general edge detection methods, such as the Sobel operator and Laplacian operator, are relatively readily affected by background noise, resulting in some false edge interference.[13] The SEM images of photoresist lines usually contain considerable noise.[14] In the process of edge recognition, the actual edges and the false edges need to be perfectly separated. Therefore, it is necessary to find a suitable method to detect the edges of patterns.

The Canny edge detection algorithm is a multilevel edge detection algorithm developed by Canny in 1986.[15] It has outstanding detection accuracy and the highest signal-to-noise ratio[16] and has been widely used in medicine,[17] cryptography, and engineering.[18] High-precision edge detection is also the key to evaluating the quality of photoresist patterns; however, the application of the Canny algorithm in the lithography field is barely reported. The basic steps of the Canny algorithm are presented as follows. Step 1: grayscale conversion. Since this algorithm can only calculate grayscale images, it is necessary to convert non-grayscale images to grayscale images. Step 2: noise reduction processing. General images contain considerable noise, which is mostly pretzel noise as well as Gaussian noise. The Canny operator is an edge detection method that comprehensively seeks the optimal compromise between anti-noise interference and accurate positioning. Gaussian filtering is generally used to remove noise. Step 3: calculation of the gradient strength and direction of each pixel and use of the first-order finite difference to calculate the gradient to obtain two matrices of partial derivatives of the image in the x and y directions. The Canny operator uses the Sobel operator as the gradient operator. Step 4: non-maximum suppression, which refines the wide edge band and only retains the processing of edge peaks. Based on the gradient direction obtained in the previous step, the neighboring pixel points of the image along the gradient direction or the inverse direction are compared and retained if they are the maximum value; otherwise, they are suppressed. Step 5: double threshold detection, the use of two thresholds to detect strong edges and weak edges. The edges higher than the high threshold are strong edges. Those between the high threshold and the low threshold are weak edges. The strong edge output represents

https://doi.org/10.1021/acsomega.2c06769
ACS Omega 2023, 8, 3992−3997

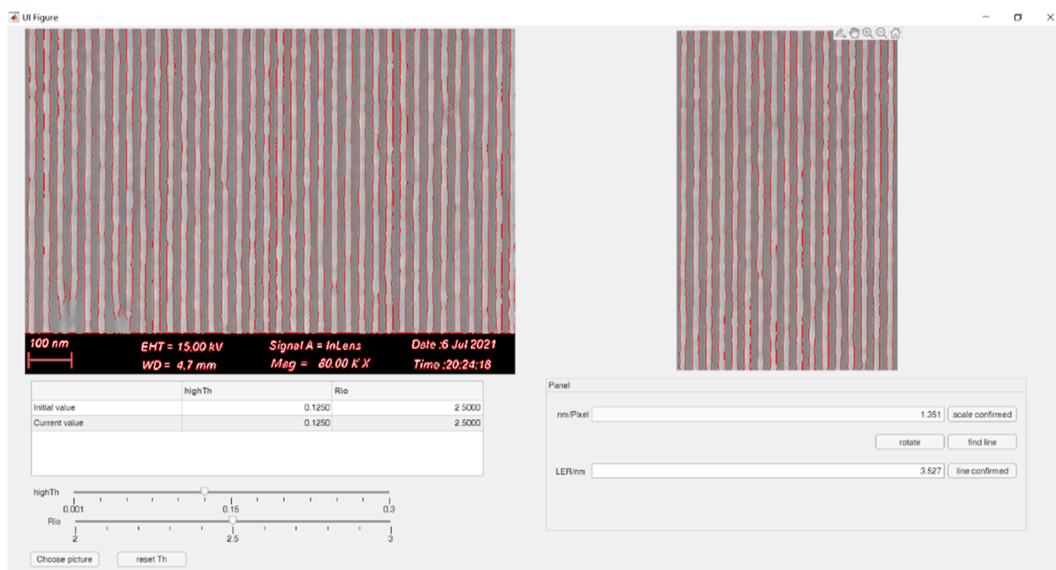

Figure 2. Edge detection of the image with 15 nm resolution and pixel size calculation in the user GUI.

true edges, while the weak edges are output only when these edges are connected to strong edges.

The noise at the bottom of the SEM image of the photoresist line is generally a discontinuous short line, and the signal intensity is also lower than the actual edge. Therefore, the method of adjusting the values of the double threshold can be used to filter out the noise. The values of the double threshold significantly affect edge detection. For some SEM images with poor quality, the initial double threshold given by the Canny algorithm in MATLAB sometimes cannot remove false edges. Therefore, in our work, we add an additional step of resizing the double threshold before stripping out the edges of the pattern. According to the coincidence between the edge and the original pattern, the optimal double threshold is determined, which can better extract the true edges.

After the edges are extracted, the coordinates of the edges need to be converted into the actual size, and then, the analysis and calculation of the LER/LWR can be performed. Because each SEM image includes a scale, our measurement software also measures the pixel length of the scale, and the extracted edge data can be converted into the actual size after simple conversion.

2.2. Amplitude Analysis and PSD Fractal Analysis.

The analysis methods for LER/LWR are mainly divided into two categories: amplitude measurement and spectrum analysis.[19] Amplitude measurement is the basic way to characterize LER, and almost all researchers use 3 times the root mean square error (RMSE) to characterize LER. The RMSE of LER is determined using eq 2.

$$\sigma_{\mathrm{LER}} = \sqrt{\frac{1}{N}\sum_{i=1}^{N}(x_j - \overline{x})^2} \tag{2}$$

where N represents the number of points taken on the edge, x_j represents the position of the jth point on the edge, and $\overline{x}$ represents the average position of N points.

The size of the RMSE can intuitively reflect the roughness of the line edge. However, this value cannot reflect the more detailed spatial information on the outline of the line edge. Even the same RMSE may correspond to different line edges. Therefore, it is also necessary to investigate the variation period of the roughness along the edge of the line. Generally, most researchers regard line roughness as noise and use PSD to investigate it.[20] The PSD can intuitively divide the roughness of an edge into different Fourier components from the frequency domain and reflect most of the information of the spatial frequency features on the edge.

The PSD function can be obtained by taking the square of the mode of the discrete Fourier amplitude of the edge position error, and eqs 3 and 4 define the relationship between the PSD of the LER and the Fourier function.[21]

$$P_n = \frac{L}{2\pi}|F_n|^2 \tag{3}$$

$$F_n = \frac{1}{N}\sum_{j=0}^{N-1}(x_j - \overline{x})\exp(-ik_n j\Delta y) \tag{4}$$

where N represents the number of points taken on the edge, x_j represents the position of the jth point on the edge, $\overline{x}$ represents the average position of N points, and Δy is the distance between the measurement points. k_n is the discrete wavenumber, which is defined by eq 5.

$$k_n = \frac{2\pi n}{L} \tag{5}$$

Generally, the signals in the middle- and low-frequency bands in the spatial frequency domain correspond to the actual roughness of the lines, while the PSD signals in the high-frequency region correspond to the white noise.[22] The main sources of white noise are statistical errors as well as systematic errors, including limited picking points and edge shrinkage caused by electron irradiation. This white noise is difficult to filter out by edge detection algorithms but can be removed by correlation model fitting. We use eq 6, a PSD model, to fit the measured data and remove the white noise. ξ is the correlation length, α is the roughness index, and Nl is the component corresponding to the white noise.[11]

$$\mathrm{PSD}(\upsilon) = \frac{\xi\sigma_{\mathrm{unbiased}}^{\ 2}}{(1+\xi^2\upsilon^2)^{1+\alpha}} + Nl \tag{6}$$

https://doi.org/10.1021/acsomega.2c06769
ACS Omega 2023, 8, 3992−3997

According to the Parseval identity, the squared sum of the coefficients after the Fourier transform of the function and the squared sum of the function values can be directly correlated.

$$\sigma_{\mathrm{p}}^{2} = \frac{2\pi}{L} \sum_{n=0}^{N-1} P_n \tag{7}$$

3. RESULTS AND DISCUSSION

Taking the novel Zr nanoparticle photoresist developed by our group as an example, we obtained periodic line patterns by EBL. Our software interface can easily select the line pattern to be tested. Figure 2 shows the edge detection after selecting the image with 15 nm line resolution, highlighting the edge lines at the detection point. The lower two sliders can adjust the high threshold and the ratio of high and low thresholds in the Canny algorithm so that the detected edge lines are consistent with the actual edge. The pixel size is obtained by using MATLAB's ocr function to identify the scale in the image and calculate it. Finally, the LER value is calculated by selecting the area to be measured from the image. The adjustment of the double threshold can effectively reduce the influence of background noise. Figure 3 shows the photoresist lines obtained by e-beam lithography using the zirconia nanoparticle photoresist. The yellow circles in Figure 3 show the effect of the high and low threshold ratios on edge detection. The high threshold of Figure 3a is 0.03, and after adjusting it to 0.14, the background noise is removed and Figure 3b is obtained. However, the ratio between the high and low thresholds of 2.0 is not appropriate, and some of the edges are not recognized, as shown in the yellow circle in Figure 3b. When the ratio is increased to 2.5, the lines are connected to get a complete edge.

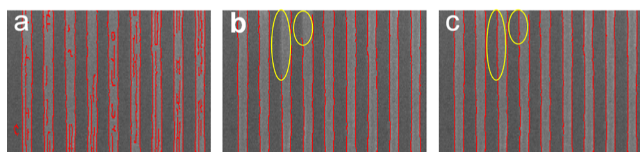

Figure 3. (a) Edges detected by the Canny algorithm with the default threshold. (b) High threshold adjusted from 0.03 to 0.14 for rejecting background noise. (c) High and low threshold ratios adjusted from 2.0 to 2.5 for connecting the line edges.

We prepared 1:1 lithographic lines with a half-period of 100 nm using an electron beam lithograph and obtained a set of images of the same area on SEM with different cycle times. After edge detection, we tested the LER calculation function with this set of lithography line SEM images. As shown in Figure 4a−e, the white noise content in the images decreases sequentially as the cycle time increases.[23] The corresponding LER and unbiased LER are calculated using eqs 2-8. The results are shown in Table 1 and Figure 4f. The PSD curves of each image are formed, as shown in Figure S1.

Table 1. LER Calculation Results for Photolithographic Lines with Different Cycle Times

image	cycle time (s)	LER (nm)	unbiased LER (nm)
A	0.37	9.8	8.1
B	0.68	9.1	8.2
C	1.3	8.9	8.1
D	2.6	8.8	8.2
E	5.2	8.7	8.2

These images correspond to the exact same photolithographic lines, and their LERs should be equal in theory. However, the LER calculated from the amplitude increases with increasing noise. It can be observed from the results (Figure 4f) that the roughness of the lines is gradually reduced as the cycle time increases, indicating that the white noise affects the roughness measurement. After the PSD fitting noise

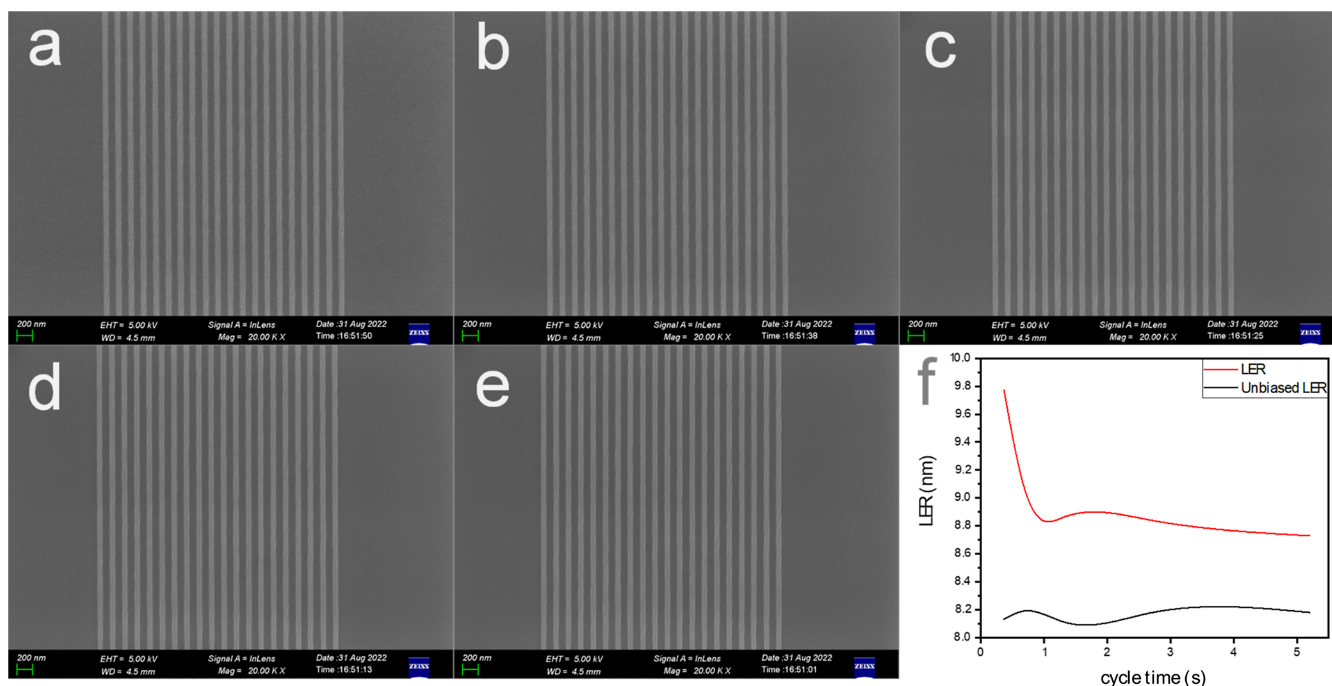

Figure 4. (a−e) Lithography images with the cycle time ranging from 0.37 to 5.2 s. (f) LER and unbiased LER of each image.

https://doi.org/10.1021/acsomega.2c06769
ACS Omega 2023, 8, 3992−3997

reduction, the roughness converges to the same value.[19] This indicates that this PSD fitting model matches the Canny edge detection algorithm and can effectively reduce the deviation caused by white noise.

4. CONCLUSIONS

In this work, we present a software for offline measurement of LER, which extracts edge points from SEM images using the Canny algorithm with adjustable double thresholding to screen out background noise. Using the extracted data, roughness parameters such as the LER of the lines can be calculated. Taking the high-resolution patterns obtained by EBL as an example, we conducted calculations using this software. It can compare the roughness of these lines, consistent with the information from the actual image. The software can extract data regarding the edge error of the lines, and using these data, PSD curves can be obtained. Fitting with a suitable PSD unbiased model can yield roughness values that eliminate white noise.

Anyone can obtain the current beta version by contacting the authors. We hope that this open-source LER measurement software can contribute to lithography research, and the software supports the extension of more unbiased PSD models to fit SEM images with different conditions.

■ ASSOCIATED CONTENT

Supporting Information

The Supporting Information is available free of charge at https://pubs.acs.org/doi/10.1021/acsomega.2c06769.

> Method of synthesizing a photoresist obtaining lithographic patterns; PSD curves of each image in Figure 4; and pseudocode of the software (PDF)

■ AUTHOR INFORMATION

Corresponding Authors

Hong Xu − *Institute of Nuclear and New Energy Technology, Tsinghua University, Beijing 100084, China;* orcid.org/0000-0001-7918-1454; Email: hongxu@tsinghua.edu.cn

Xiangming He − *Institute of Nuclear and New Energy Technology, Tsinghua University, Beijing 100084, China;* orcid.org/0000-0001-7146-4097; Email: hexm@tsinghua.edu.cn

Authors

Ziyu Hu − *Institute of Nuclear and New Energy Technology, Tsinghua University, Beijing 100084, China*

Rongbo Zhao − *Institute of Nuclear and New Energy Technology, Tsinghua University, Beijing 100084, China*

Xiaolin Wang − *Institute of Nuclear and New Energy Technology, Tsinghua University, Beijing 100084, China*

Peipei Tao − *Institute of Nuclear and New Energy Technology, Tsinghua University, Beijing 100084, China*

Qianqian Wang − *Institute of Nuclear and New Energy Technology, Tsinghua University, Beijing 100084, China*

Yimeng Wang − *Institute of Nuclear and New Energy Technology, Tsinghua University, Beijing 100084, China*

Complete contact information is available at: https://pubs.acs.org/10.1021/acsomega.2c06769

Notes

The authors declare no competing financial interest.

■ ACKNOWLEDGMENTS

The authors acknowledge the financial support from the National Natural Science Foundation of China (52073161), the Tsinghua University Initiative Scientific Research Program (no. 2021Z11GHX010), and the Beijing Municipal Science & Technology Commission, Administrative Commission of Zhongguancun Science Park (no. Z211100004821008).

■ REFERENCES

(1) Kaestner, M.; Rangelow, I. W. Scanning probe lithography on calixarene towards single-digit nanometer fabrication. *Int. J. Extreme Manuf.* **2020**, *2*, 032005.

(2) Lee, J. L.; Shin, J.-Y.; Kim, J.; Woo, H.-W.; Cho, S.-G.; Han, H.-K.; Moon, W.-S.; Moon, J.-T. Effect of line-edge roughness (LER) and line-width roughness (LWR) on sub-100-nm device performance. *Proc. SPIE* **2004**, *5376*, 426−433.

(3) Gustin, C.; Leunissen, L. H. A.; Mercha, A.; Decoutere, S.; Lorusso, G. Impact of line width roughness on the matching performances of next-generation devices. *Thin Solid Films* **2008**, *516*, 3690−3696.

(4) Buitrago, E.; Nagahara, S.; Yildirim, O.; Nakagawa, H.; Tagawa, S.; Meeuwissen, M.; Nagai, T.; Naruoka, T.; Verspaget, C.; Hoefnagels, R.; et al. Sensitivity enhancement of chemically amplified resists and performance study using extreme ultraviolet interference lithography. *J. Micro/Nanolithogr., MEMS, MOEMS* **2016**, *15*, 033502.

(5) Azarnouche, L.; Pargon, E.; Menguelti, K.; Fouchier, M.; Fuard, D.; Gouraud, P.; Verove, C.; Joubert, O. Unbiased line width roughness measurements with critical dimension scanning electron microscopy and critical dimension atomic force microscopy. *J. Appl. Phys.* **2012**, *111*, 084318.

(6) Li, L.; Chakrabarty, S.; Jiang, J.; Zhang, B.; Ober, C.; Giannelis, E. P. Solubility studies of inorganic-organic hybrid nanoparticle photoresists with different surface functional groups. *Nanoscale* **2016**, *8*, 1338−1343.

(7) Xiang, Q.; Chen, Y.; Wang, Y.; Zheng, M.; Li, Z.; Peng, W.; Zhou, Y.; Feng, B.; Chen, Y.; Duan, H. Low-voltage-exposure-enabled hydrogen silsesquioxane bilayer-like process for three-dimensional nanofabrication. *Nanotechnology* **2016**, *27*, 254002.

(8) Chen, Y.; Shu, Z.; Zhang, S.; Zeng, P.; Liang, H.; Zheng, M.; Duan, H. Sub-10 nm fabrication: methods and applications. *Int. J. Extreme Manuf.* **2021**, *3*, 032002.

(9) Patsis, G. P.; Constantoudis, V.; Tserepi, A.; Gogolides, E.; Grozev, G. Quantification of line-edge roughness of photoresists. I. A comparison between off-line and on-line analysis of top-down scanning electron microscopy images. *J. Vac. Sci. Technol., B: Microelectron. Nanometer Struct.* **2003**, *21*, 1008−1018.

(10) Yazgi, S. G.; Ivanov, T.; Holz, M.; Rangelow, I. W.; Alaca, B. E. Line edge roughness metrology software. *J. Vac. Sci. Technol., B: Nanotechnol. Microelectron.: Mater., Process., Meas., Phenom.* **2020**, *38*, 012602.

(11) Mochi, I.; Vockenhuber, M.; Allenet, T. P.; Ekinci, Y.; Renwick, S. P.; Preil, M. E. Open-source software for SEM metrology. *Proc. SPIE* **2020**, *11518*, 115180G.

(12) Seiler, H. Secondary electron emission in the scanning electron microscope. *J. Appl. Phys.* **1983**, *54*, R1−R18.

(13) Basu, M. Gaussian-based edge-detection methods-a survey. *J. Vac. Sci. Technol., B: Nanotechnol. Microelectron.: Mater., Process., Meas., Phenom.* **2002**, *32*, 252−260.

(14) Nishida, A. Statistical- and image-noise effects on experimental spectrum of line-edge and line-width roughness. *J. Micro/Nanolithogr., MEMS, MOEMS* **2010**, *9*, 041210.

(15) Canny, J. A computational approach to edge detection. *IEEE Trans. Pattern Anal. Mach. Intell.* **1986**, *8*, 679−698.

(16) Lu, Y.; Duanmu, L.; Zhai, Z.; Wang, Z. Application and improvement of Canny edge-detection algorithm for exterior wall hollowing detection using infrared thermal images. *Energy Build.* **2022**, *274*, 112421.

(17) Hu, R.; Li, M.; Xu, H.; Zhao, H. M. Research and Application of Key Technologies for Medical Image Intelligence Knowledge Discovery and Data Processing. *Int. J. Pattern Recognit. Artif. Intell.* **2020**, *34*, 2057005.
(18) Gokhale, A. M.; Yang, S. Application of image processing for simulation of mechanical response of multi-length scale microstructures of engineering alloys. *Metall. Mater. Trans. A* **1999**, *30*, 2369−2381.
(19) Constantoudis, V.; Patsis, G. P.; Leunissen, L. H. A.; Gogolides, E. Line edge roughness and critical dimension variation: Fractal characterization and comparison using model functions. *J. Vac. Sci. Technol., B: Nanotechnol. Microelectron.: Mater., Process., Meas., Phenom.* **2004**, *22*, 1974−1981.
(20) Ohfuji, W.; Endo, T.; Morimoto, M.; Morimoto, H. Theoretical analysis of line-edge roughness using FFT techniques. *Proc. SPIE* **1999**, *3678*, 32−38.
(21) Verduin, T.; Kruit, P.; Hagen, C. W. Determination of line edge roughness in low-dose top-down scanning electron microscopy images. *J. Micro/Nanolithogr., MEMS, MOEMS* **2014**, *13*, 033009.
(22) Kirchner, J. W. Aliasing in1/fαnoise spectra: Origins, consequences, and remedies. *Phys. Rev. E: Stat., Nonlinear, Soft Matter Phys.* **2005**, *71*, 066110.
(23) Lorusso, G. F.; Rutigliani, V.; Van Roey, F.; Mack, C. A. Unbiased roughness measurements: Subtracting out SEM effects, part 2. *J. Vac. Sci. Technol., B: Nanotechnol. Microelectron.: Mater., Process., Meas., Phenom.* **2018**, *36*, 06J503.

https://doi.org/10.1021/acsomega.2c06769
ACS Omega 2023, 8, 3992−3997